

FILTECH 2011

CONFERENCE PROCEEDINGS

VOLUME I

CONTENT VOLUME I

Scientific Committee	I-2
Session Survey	I-3
Conference Programme	I-4
Keyword List (Session Indicator)	I-15
Session Chairmen	I-17
Survey Lectures	I-19
Papers L-Sessions	I-94
Keyword List (Page Indicator)	I-668

CONTENT VOLUME II

Scientific Committee	II-2
Session Survey	II-3
Conference Programme	II-4
Keyword List (Session Indicator)	I-15
Session Chairmen	II-17
Papers G-Sessions	II-19
Papers M-Sessions	II-465
Keyword List (Page Indicator)	II-628

Conference Dates:

March 22 – 24, 2011

Venue:

Rhein-Main-Hallen · Rheinstr. 20 · 65028 Wiesbaden · Germany

Organizer:

Filtech Exhibitions Germany
PO Box 1225 · 40637 Meerbusch – Germany
phone: +49 (0) 2132 93 57 60
fax: +49 (0) 2132 93 57 62
e-mail: Info@Filtech.de
web: www.Filtech.de

ISBN 978-3-941655-011-0

NUMERICAL SIMULATION OF AGGLOMERATION AND FILTRATION OF COLLOIDAL SUSPENSIONS

F. Keller, C. Eichholz, B. Schäfer and H. Nirschl
Karlsruhe Institute of Technology, Institute of Mechanical Process Engineering and
Mechanics, Straße am Forum 8, 76131 Karlsruhe.

Abstract

Numerical simulations have become an essential tool to gain further insights into the behaviour of colloidal systems. Thereby it is necessary to consider not only the fluid flow but also the electrostatic interactions between the colloidal particles. In this article we present numerical studies for the simulation of colloidal systems during agglomeration and filtration to give further insight in the formation and permeability of colloidal filter cakes. First we present a direct numerical simulation study based on an overlay grid technique, which completely resolves the particles and allows the study of the diverse microscopic effects of the double layer interactions for a small number of particles. Especially the influence of the ionic strength and the volume fraction on the flow through a packed bed is investigated. For higher particle numbers we present a combined stochastic rotation dynamics (SRD) and a discrete element method (DEM) for an efficient simulation of the agglomeration and cake formation process. Further, we investigate the dependence of the structure and the permeability of the filter cake on the agglomeration of the particles. A promising method to reduce the flow resistance of filter cakes is the magnetic field enhanced cake filtration which results from combination of classical cake filtration and magnetic field driven separation. We present a numerical study of the cake filtration and growth by means of the discrete element method.

Keywords

Agglomeration, Filtration, Colloids, Numerical Simulation

1. Introduction

Colloidal particles, i.e. particles with a size below 1 μm , play an important role in a wide range of applications, like in chemical and biological industry and science. The production of these particles often takes place in electrolyte solutions, where they acquire a non-zero surface charge, which leads to the formation of an electric double layer around the particles. The interactions between the charged particles itself and their electric double layers is classically described by the famous DLVO-theory, which has the drawback that only pair wise interactions are considered and that the deformations of the double layers due to the surrounding fluid flow are neglected. In the present paper numerical simulations are used to give further insight in the underlying physical principles. For a small number of particles direct numerical simulation can be used, where the geometry of the particles is fully resolved by a overlay grid technique. In this way all nonlinear interactions between the particles are

included in the simulation. Especially we investigate the electrokinetic interactions in periodic cubic arrays. By increasing the number of particles, it is necessary to overcome the huge computational costs of a direct numerical simulation. Therefore we use a combination of a stochastic rotation dynamics (SRD), which is a coarse grained fluid description, and a discrete element method (DEM) including the DLVO potential. We use our model to simulate cake filtration and predict the permeability of the filter cakes depending on the compressive load, the particle size and the agglomeration of the particles. We show that our results agree qualitatively with experimental data obtained from colloidal boehmite suspensions. It is known that the permeability of the filter cake increases with decreasing particle size and the mechanical dewatering becomes more and more difficult. One possibility to improve the filtration kinetics is the process of magnetic field enhanced cake filtration, which results from the combination of classical cake filtration and magnetic field driven separation (Fuchs et al. [3], Eichholz et al. [2]). Experimental results prove that different magnetic field effects influence the filtration process positively. Therefore DEM simulations are performed to give a deeper understanding in the mechanisms of structuring effects of the filter cake and the interaction of magnetic, hydrodynamic and mass forces.

2. Direct Numerical Simulation of the flow through colloidal packed beds

If we consider the flow of a Newtonian electrolyte solution through a filter cake consisting of charged colloidal particles, not only the fluid flow but also the electrochemical interactions via the electric double layers have to be considered. By employing direct numerical simulations all these effects can be taken into account. Despite the Navier-Stokes equation, we additionally have to consider the electric field that develops around the particles as well as the ion distributions in the electrolyte solution. This leads to the Stokes-Poisson-Nernst-Planck system, a system coupled partial differential equations for the fluid velocity and pressure (u, p) , the electrostatic potential ψ and the concentration of each ion species in the electrolyte solution n_i ,

$$-\nabla p + \eta \Delta u - \rho_e \nabla \psi = 0, \quad (1)$$

$$\nabla \cdot u = 0, \quad (2)$$

$$-\Delta \psi = \frac{1}{\varepsilon} \rho_e, \quad (3)$$

$$u \cdot \nabla n_i - \frac{k_B T}{\lambda_i} \Delta n_i - \frac{e}{\lambda_i} \nabla \cdot (z_i n_i \nabla \psi) = 0, \quad (4)$$

with the fluid viscosity η , the charge density ρ_e , the permittivity ε of the solvent, the Boltzmann constant k_B and the temperature T . Further the ion species i is characterized by its drag coefficient λ_i and its valency z_i . The solution of the above system for a large number of particles is a time-consuming task, which can be reduced by introducing periodic boundary conditions. In this article we especially consider ordered arrays that can be represented by a periodic unit cell, see figure 1. In the simplest case, a single particle can represent the filter cake. We solve these equations by applying the Chimera grid technique, which is a conceptually simple

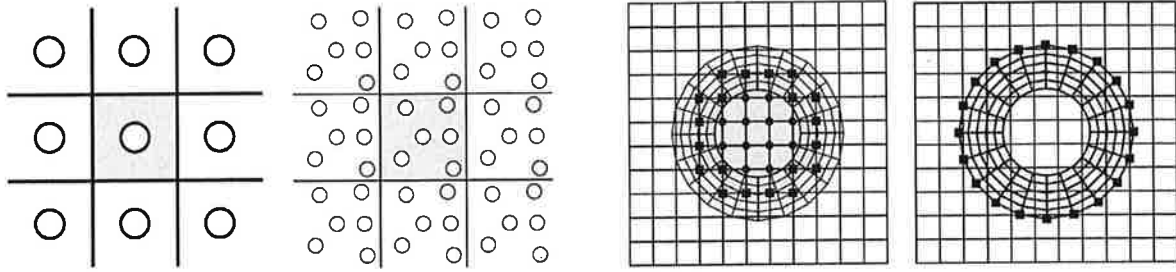


Figure 1. Left: Periodic unit cell representing the filter cake. Right: Overlapping grids with interpolation points for the Chimera technique.

domain decomposition approach using overlapping grids (see e.g. Nirschl et al. [4]). While we use a main coarse Cartesian grid for the periodic unit cell, we attach a fine body-fitted grid for every particle, see figure 1, to resolve the steep gradients that occur in the electric potential and in the ion concentrations near the particle surface. Information between the grids is transferred via interpolation routines. The Chimera grid method offers the advantage that multi-particle systems and non-spherical particles can be easily handled. For the solution on the main and body-fitted grids, we use the finite element method with the possibility of hanging nodes. Therefore we employ the finite element package deal.II, see Bangerth [1]. In the following, we investigate the flow through two special periodic arrays of charged spheres. First we use the simple cubic array (SC), which is shown on the left of figure 2. This array consists simply of one particle at the center the periodic unit length. Further we consider the body-centered cubic array (BCC) shown on the right in figure 2, with one particle at the center and additionally one particle at each vertex of the unit cell. For all our computations we have used the electrolyte KCl, a pressure drop of $1e5$ Pa/mm, particles with a radius of 300 nm and a zeta potential of $\zeta = 77,7$ mV. Due to the fluid flow the double layer is distorted and the force on the particle is no longer of pure hydrodynamical but also of electrical nature, which results in a change of the permeability of the filter cake. We use the following scaled permeability,

$$K^* = \frac{K}{d^2} \cdot \frac{\phi^2}{(1-\phi)^3},$$

where

$$K = \frac{\dot{V}\eta}{|\Delta p / L|L^2}$$

is the permeability of the filter cake. We use a constant volume fraction of 0.303 which corresponds to a unit cell length of $L = 1.2d$ in a simple cubic grid. We will concentrate on the influence of the ionic strength which has an effect on the double layer thickness and thus on the ratio κd . In figure 3 the dependence of the dimensionless permeability on the double layer thickness is shown.

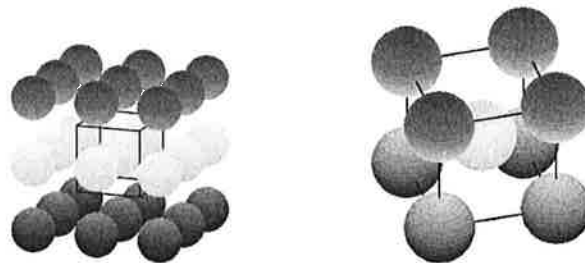


Figure 2. Left: Simple Cubic Array (SC). Right: Body-centered cubic array (BCC).

For $\kappa d = 0$, which corresponds to an infinitely dilute solution, we recover the permeabilities of the pure fluid. For increasing double layer thickness, we see for both arrays, that the permeabilities decrease due to the distortion of the double layer. It can also be seen that the permeability of the simple cubic grid is higher than the permeability of the body-centered cubic array. It is expected, that the permeabilities increase again for larger values of the Debye length.

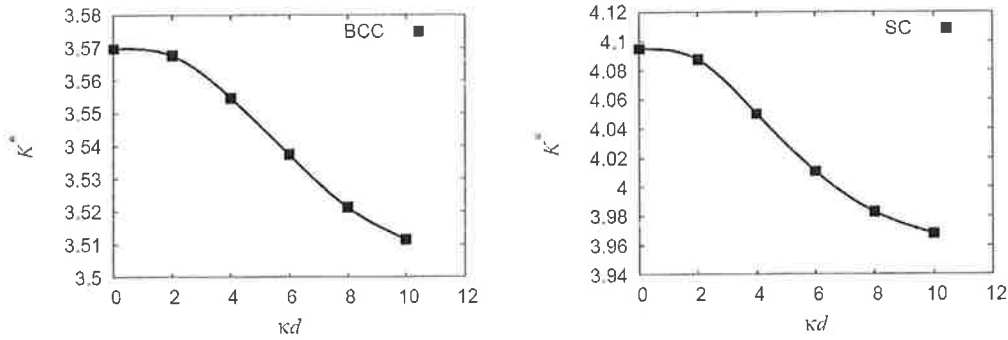


Figure 3. Scaled permeabilities of the body-centered (left) and simple cubic arrays (right) in dependence on the double layer thickness.

3. Coupling of stochastic rotation dynamics and DEM

As described in the preceding section, direct numerical simulation is well suited for the investigation of details in double layer interactions but is restricted to a small number of particles due to its high numerical costs. Therefore we propose a coupling of a stochastic rotation dynamics for a coarse grained simulation of the fluid and a discrete element method for the efficient handling of larger numbers of particles.

The stochastic rotation dynamics (SRD) method has the advantage that it has low demands for computational time and that it intrinsically contains fluctuations. It is based on the calculation of the continuous positions of virtual fluid particle (SRD particles). Since these virtual fluid particles are treated as pointlike, momentum is exchanged in a collective interaction step: the SRD particles are sorted into cubic cells. Within each cell, the relative velocities of the particles with respect to their average velocity are rotated. The rotation matrix is stochastically chosen for each cell and time step from a set of six possible rotations by $+90^\circ$ or -90° around the three coordinate axes. In this way it is guaranteed that, within each cell, the total mass, momentum and energy is conserved. The motion of the colloidal particles is calculated by a discrete element method. The basic idea of the discrete element method is to solve Newton's equations of motion for each colloidal particle. For a colloidal particle i these read as

$$m_i \frac{dv_i}{dt} = F_i,$$

$$J_i \frac{d\omega_i}{dt} = T_i,$$

with the mass m_i and the inertia tensor J_i of the particle, the velocity and angular velocity v_i and ω_i , as well as the total force and momentum F_i and T_i acting on the particle. We use the well-known DLVO interaction potential, including electrostatic repulsion, van der Waals attraction and Born repulsion. In order to reduce the potential gradients and thus to expand the simulation time step, the Born potential, which prevents the particles from overlapping is replaced by the less steep Hertz

potential. So we use the following interaction forces, which can be found in Russel et al. [5],

$$F_{elec,ij} = -\pi\epsilon \left(\frac{4k_B T}{e} \tanh\left(\frac{ze\zeta}{4k_B T}\right) \right)^2 \cdot \left(\frac{1}{r_{ij}^2} + \frac{\kappa}{r_{ij}} \right) \cdot \exp(-\kappa(r_{ij} - d_p)) \cdot n_{ij},$$

$$F_{vdW,ij} = \frac{H_0}{6} r_{ij} d_p^2 \left(\frac{1}{r_{ij}^2 - d_p^2} - \frac{1}{r_{ij}^2} \right)^2 \cdot n_{ij},$$

$$F_{Hertz,ij} = -K_{Hertz} \cdot (d_p - d)^{1.5} \cdot n_{ij},$$

with the unit vector n_{ij} pointing from the center of particle i to particle j , the distance r_{ij} between the particles and the Hamaker constant H_0 . Further we use the Hertz constant $K_{Hertz} = 0.25$. Although SRD is a hydrodynamic simulation method, it does not fully reproduce this behavior for inter-particle distances below one particle diameter because the fluid in the SRD simulation is coarse grained and thus has a lower resolution. For particles being closer, this shortcoming is corrected by the dissipative lubrication force

$$F_{lub,ij} = -(\dot{x}_i - \dot{x}_j) \frac{6\pi c_{lub} \eta}{r_{ij} - d_p} \left(\frac{d_p}{4} \right)^2 n_{ij}.$$

The lubrication constant c_{lub} takes into account that the dissipation is partly reproduced by the hydrodynamics. We use a value of $c_{lub} = 0.2$.

We use the above described simulation method to investigate the influences of the particle size, the particle charge and the ionic strength on the resulting agglomerate structure and on the filtration. Especially we determine the porosity and the permeability of the filter cake. The results are shown in figure 4. Of course, a higher pressure leads to a lower porosity of the filter cake. The compressibility of the filter cake strongly depends on the internal structure: a stabilized suspension leads to a dense packing even at low compressive loads, while the loose structure resulting from agglomerated particles can be easily compressed by rearrangement of the particles, so that the agglomerates can be considered as deformable particles. The compressibility is negligible at an ionic strength of 0.1 mol/L, where the particles are in very close contact. The compressibility increases again for lower ionic strengths,

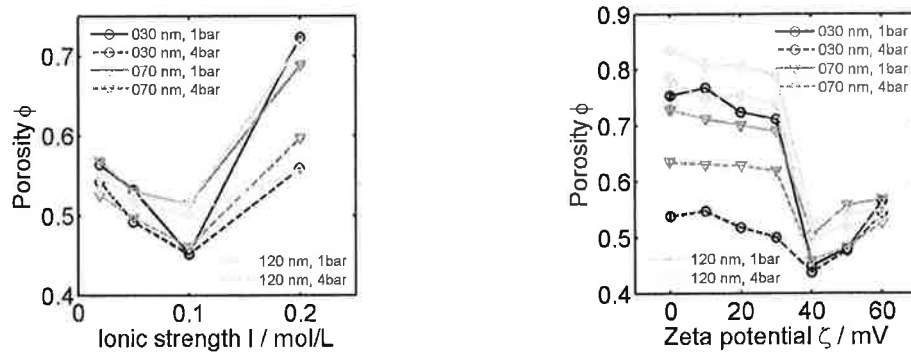


Figure 4. Left: Porosity of the filter cakes depending on the ionic strength of the suspension for different particle diameters and for different compressive loads. Right: Porosity of the filter cakes depending on the zeta potential of the particles for different particle diameters and for different compressive loads.

since the electric repulsion becomes stronger such that the particles in the resulting dense bed are at a larger distance to each other. By increasing the ionic strength, particles agglomerate leading to a higher porosity. The porosity of the filter cakes also depends on the zeta potential of the particles, see figure 4. At low zeta potentials, the porosity is relatively high for all particle diameters and for all compressive loads because the particles are agglomerated, which is also observed in the experiments. At a zeta potential of 40 mV, the Coulomb repulsion prevents agglomeration, causing a lower porosity. A further increase of the zeta potential increases the repulsion and thus the distance between the particles. This is in analogy to the case of decreasing the ionic strength. Further the permeabilities of the filter cakes have been calculated using the Lattice Boltzmann method (LBM). The simulations reveal that, for each particles size, the permeability of a packed bed is an exponential function of its porosity which itself depends on the zeta potential, the ionic strength, and the compressive loads (see figure 5). A significant deviation from the exponential relation between the porosity and the permeability is found only for the 30 nm particles, where the simulated permeabilities are too high for porosities around 0.55. This indicates a stronger influence of the pore size heterogeneity on the permeability for smaller particles. Similar exponential relations between the porosity and the permeability are found in the experiments (Schäfer and Nirschl [6]) on the permeability of filter cakes consisting of colloidal boehmite particles, see figure 5.

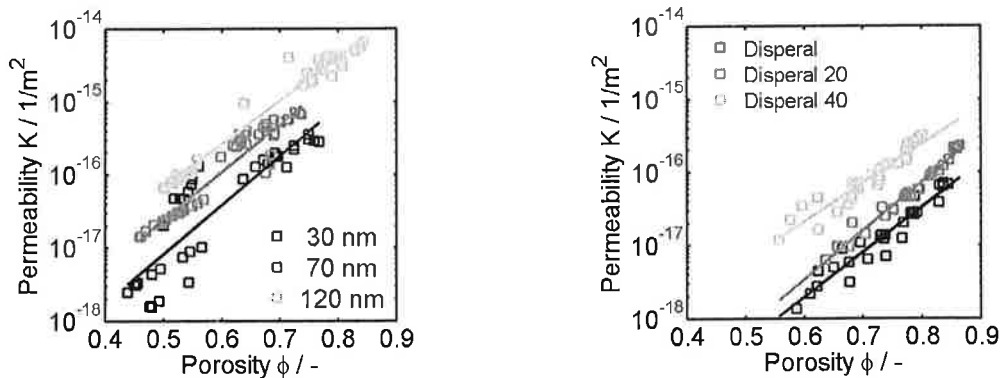


Figure 5. Left: Permeability depending on the porosity for different particle diameters as resulting from the simulations. Right: Permeability depending on the porosity for different particle diameters as resulting from experiments.

4. DEM simulations of magnetic enhanced cake filtration

As seen in the previous sections, filter cakes consisting of colloidal particles show low permeabilities and therefore high resistances. A promising method to lower these resistances is the magnetic enhanced cake filtration. Therein the fact is used, that particles in an inhomogeneous magnetic field experience a magnetic force, which gives the possibility to decouple solid and liquid phase motion. In case of counter wise orientation of differential pressure and magnetic force, this leads to a decrease of the rate of cake formation, implying a smaller packed bed that the liquid has to drain and thus a reduction in filtration resistance. The discrete element method is used to give further insight into this process. In addition to the forces introduced in the preceding section we have to consider the following magnetic forces

$$F_{m,ext} = V\rho M\nabla B,$$

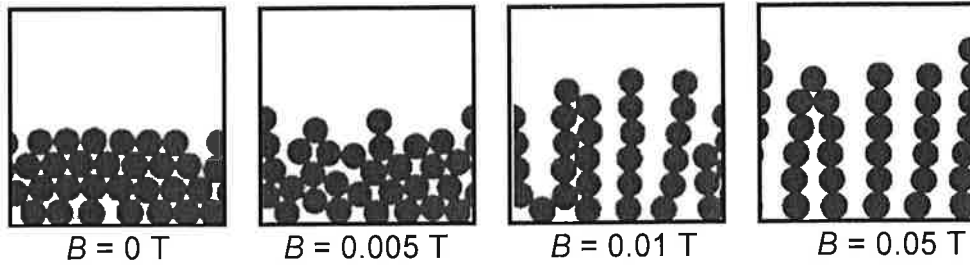


Figure 6. Final particle packing for different magnetic field strengths.

$$F_{m,dip,ij} = \frac{3\pi\mu_0\rho^2 d_p^6}{144} \cdot \frac{M_i \cdot M_j}{r_{ij}^4} \cdot \left\{ (m_i \cdot m_j) n_{ij} + 5 (m_i \cdot n_{ij}) \times (m_j \cdot n_{ij}) n_{ij} - (m_j \cdot n_{ij}) m_i - (m_i \cdot n_{ij}) m_j \right\},$$

with the permeability μ_0 , the magnetic field strength B , the magnetization M and the magnetic moment m of a particle. In a first step the DLVO potential is neglected and we investigate only the influence of an applied external magnetic field. Figure 7 shows the effect of different magnitudes of the external field on the structure of the filter cake. Since the DLVO potential is not considered the densest packing of spheres is obtained for the case $B = 0T$ which corresponds to classical filtration. By increasing the magnetic field strength the filter cake changes to a looser structure leading to a lower porosity of the filter cake and hence to a lower filter resistance. Eichholz et al. [2] showed that an energy ration E_s for the quantitative analysis of the cake structure formed under the influence of a magnetic field can be used, which is defined by the following expression,

$$E_s = \frac{E_{hyd}}{E_{m,dip}} = \frac{432 \eta v}{\mu_0 \rho^2 M^2 d}.$$

Thereby we have introduced the drag potential E_{hyd} which defines the energy that is needed to lift one particle against the drag force by one particle diameter and the magnetic dipole energy $E_{m,dip}$ which is the repulsive energy between two particles in contact perpendicular to the external field direction. For $E_s < 1$ the structure is strongly ordered, for $1 < E_s < 10$ only partly ordered and we can assume an unstructured bed if $E_s > 10$. So this parameter can serve as a tool to compare the

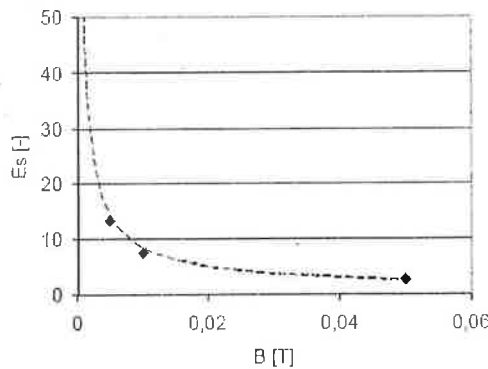


Figure 7. Structure parameter E_s as a function of the applied magnetic field.

regimes of experimental and calculated results. In figure 7 we see the calculated structure parameter from the simulations. The principle devolution correlates with experimental results, see Eichholz et al. [2].

4. Conclusions

In this article we have presented different numerical methods for the simulation of colloidal particles. We have shown the influence of the ionic strength and the volume fraction on the permeability of periodic arrays of charged spheres. A discrete element method coupled with a stochastic rotation dynamics method has been employed to investigate the agglomeration and cake filtration. Special attendance has been paid to the porosity and permeability and their dependence on the zeta potential as well as on the ionic strength. Finally we presented a discrete element method for the simulation of magnetic field enhanced cake filtration showing the dependence of the cake structure on the magnetic field strength.

5. Acknowledgements

We thank the Deutsche Forschungsgemeinschaft (DFG) for supporting the current research under the number NI 414/4-1 and within the priority program SPP 1164.

References

- [1] Bangerth, W., Hartmann, R. & Kanschat G., 2007, deal.II – a general-purpose object-oriented finite element library. *ACM Trans. Math. Softw.* 33(4), Article 24.
- [2] Eichholz, C., Stolarski, M., Goertz, V., and Nirschl, H., 2008, Magnetic field enhanced cake filtration of superparamagnetic PVAc-particles, *Chemical Engineering Science* 63(12), 3193-3200.
- [3] Fuchs, B., Stolarski, M., Stahl, W. and Nirschl, H., 2006, Magnetic field enhanced cake filtration, *Filtration* 6(4), 333-339.
- [4] Nirschl, H., Dwyer, H. A., Denk, V., 1995, Three-dimensional calculations of the simple shear flow around a single particle between two moving walls, *Journal of Fluid Mechanics*, 283, 273-285.
- [5] Russel, W. B., Saville, D. A., Schowalter, W. R., 1999, *Colloidal dispersions*, Cambridge Univ. Press.
- [6] Schäfer, B. and Nirschl, H., 2008, Physicochemical influences on electrohydrodynamic transport in compressible packed beds of colloidal boehmite particles, *Journal of Colloid and Interface Science* 318(2), 457-462.